Journal of Machine Engineering, 2022, Vol. 22, No. 4, 43–53
ISSN 1895-7595 (Print) ISSN 2391-8071 (Online)

Received: *19 October 2022* / Accepted: *30 November 2022* / Published online: *06 December 2022*

Cr_3C_2 – NiCr, plasma spraying, coating, optimization, E355 alloy steel

Thao Xuan DANG*[1]
Nguyen Hong SON[1]
Pham Duc CUONG[2]

RESEARCH ON OPTIMIZING SPRAY PARAMETERS FOR Cr3C2 – NiCr COATING CREATED ON ALLOY STEEL BY PLASMA SPRAYING TECHNIQUE

In this work, Cr_3C_2-NiCr ceramic coating with NiCr content of 30% was created on E355 (St 52-3)/1.0060 alloy steel substrate by air plasma thermal spraying (APS) method. The adhesion, tensile strength of the coating were studied in relation to spray parameters including current intensity, powder feed rate, and stand-off distance according to experimental planning. Experiments were designed based on Central Composite Design method. The adhesion and tensile strength of the coatings were measured by a tensile-compression machine. Analysis of variance (ANOVA) were used to build regression functions expressing the relationship between each property and spray parameters. The experimental results showed that those spray parameters significantly influence the properties of the coating. ANOVA results indicated that the spray parameters have different influences for each coating properties. In addition, regression model of the properties gives prediction results very close to experimental results. The optimization problem was solved in order to achieve the maximum value of adhesion and tensile strength of the coating. Values of the spray parameters for Cr_3C_2 – NiCr coating to achieve the above criteria have been determined and proposed in this study.

1. INTRODUCTION

The Cr_3C_2 – NiCr ceramic coatings attract attention from researchers due to their super properties such as high hardness, low friction coefficient and good corrosion-wear resistance [1–6]. The thermal conductivity of the Cr_3C_2 – NiCr plasma coating is reported increasing as the coating is heat treated at 980°C [7]. Thus, the Cr_3C_2 – NiCr coatings are widely used for machine parts and components that work under high temperature (up to 800 – 900ºC) and in corrosive and abrasive environments [8]. High wear resistance, of the Cr_3C_2 – NiCr coating, the NiCr alloy component serves as a corrosion resistance, while the Cr_3C_2 is considered as a hard phase assuring wear resistance. In addition, it is reported that the NiCr component reduces the porosity and microcracks of the coating and supports the easy and fast resurfacing when the coating is worn out [9].

[1] Faculty of Mechanical Engineering, Hanoi University of Industry, Hanoi City, Vietnam
[2] HaUI Institute of Technology, Hanoi University of Industry, Hanoi City, Vietnam
* E-mail: dangxuanthao@haui.edu.vn
https:/doi.org/10.36897/jme/157047

It is well known that plasma spraying is one of the most versatile and advantageous methods used, characterized by high energy density (10^6–10^7 Jm^{-3}) and heat flux (10^7–10^9 Wm^{-2}). This is important to completely melt high-melting powders to create coatings like ceramics. There are many factors affecting the formation and quality of a thermal coating such as: the coating and substrate materials, the state of the substrate surface before spraying, spraying condition, especially the spray technology parameters. In the air plasma spraying method, plasma current intensity, powder feed rate, and stand-off distance are considered as the most influential parameters to properties and quality of the coating [10–14].

Georg Mauer et al conducted research to improve plasma coating quality. The experiments were carried out by APS method with spraying parameters including input power of 39.4 kW, injection current of 600 A, Ar gas flow of 40 slpm and Hydrogen gas flow of 10 slpm; powder feed rate was 4.5 g/min along with spray angle and spray distance was about 90° and 80 mm, respectively. The results showed that, the most important parameter to improve the powder spraying process was the carrier gas flow, however it must be adjusted carefully to achieve optimum heat transfer and momentum. On the other hand, the highest particle temperature was achieved when the particles were injected deep enough to the plasma core region [15].

In another experiment by Bisson et al also showed the effect of voltage fluctuations on temperature and velocity [16]. In our previous work [14], the influence of surface roughness and plasma current on adhesion of Cr_3C_2 – 30%NiCr coating on E355 (St 52–3)/1.0060 steel was studied. From the results, value of roughness with which the adhesion achieved high was proposed and used in this study.

However, research on optimizing spray parameters for coating process is still very limited, especially research on multi-objective optimization according to some properties of Cr_3C_2 – NiCr plasma coating. In this study, we created Cr_3C_2 – NiCr coating with NiCr content of 30% on E355 (St 52–3)/1.0060 steel using air plasma spraying technique. Effects of spray parameters including current intensity, powder feed rate, stand-off distance on coating properties are studied under viewpoint of experimental planning. Experiments were carried out based on the Central Composite Design (CCD) method. Analysis of variance was used to build regression functions expressing the relationship between coating properties and the spray parameters. Finally, optimization was performed according to property criteria of the coating including adhesion strength and tensile strength, on the basis of which optimal values of the spray parameters were proposed.

2. EXPERIMENTAL PROCESS AND EVALUATION METHOD

2.1. COATING MATERIAL

Coating sample: Alloy steel E355 (St 52-3) /1.0060 is used for metal substrate because this alloy steel is commonly used in industrial machine parts working at wear and temperature conditions. The coated sample surface is cleaned and roughened by abrasive blasting. The roughness of the sample (Rz ~ 71 μm) for best adhesion is given [14].

Coating powder: Cr_3C_2 – 30%NiCr powder (Sulzer Metco – Singapore) is chosen for use in this study, Cr_3C_2 – 30%NiCr particles have an average diameter of (–30/+5 μm) with its chemical composition: C ≤ 0.2%, Si ≤ 0.5%, NiCr 29.5% and Cr_3C_2 69.8%.

2.2. PLASMA COATING PROCESS

The spraying process is carried out on plasma spraying system 3710-PRAXAIR-TAFA (USA) with spray gun SG-100. The coating thickness after the process is ($1^{+0.2}_{0}$ mm) as shown in Fig. 1. In this study, the experiments are designed according to Central Composite Design method with 2^k factorial experiments (coded as –1 and +1), 6 central points (coded as 0) and 2k axial points (placed at $-\alpha$ and $+\alpha$, where $\alpha = \sqrt[4]{2^3} = 1.682$) [17]. The values of each input at all the levels are shown in Table 1.

Table 1. Levels of parameters

Parameters	Symbols	Unit	Levels				
			$-\alpha$	–1	0	1	$+\alpha$
Current intensity	I_s	A	381.8	450	550	650	718.2
Powder feed rate	m_s	g/min	13.18	20	30	40	46.82
Stand-off distance	L_s	mm	92.72	120	160	200	227.28

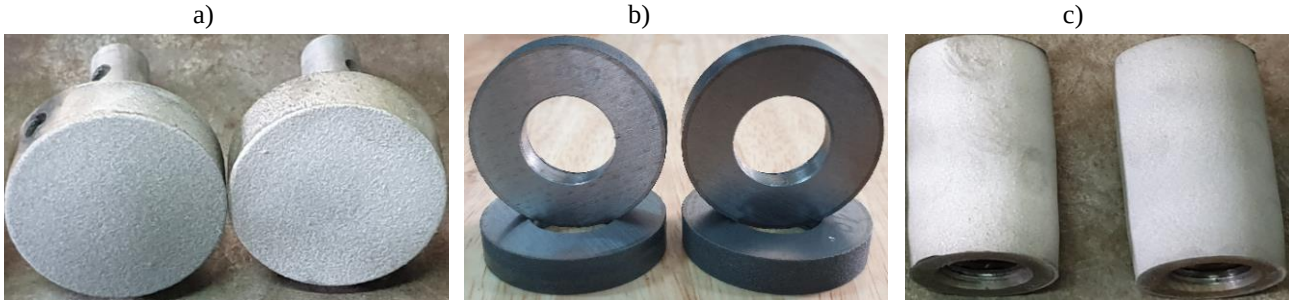

Fig. 1. Specimens with coatings: a) adhesion strength testing specimen, b) shear adhesion strength testing specimen, c) tensile strength testing specimen

2.3. EVALUATION METHODS

Measurements are determined on each sample corresponding to the schematic diagrams as shown in Fig. 2. In the study, the output parameters (σ_{As}, τ_{Sa} and σ_{Ts}) are defined using a tensile-compression tester (Model BESTUTM 500HH, Korea), the result is calculated applying formula (1), where F is the coating surface area and P is the tensile or compressive force that separates or breaks the coating as shown in Fig. 3.

$$\sigma(\tau) = \frac{P}{F}, \quad \text{(MPa)}. \tag{1}$$

For each set of spray parameters, samples were generated, and measurements were made at least 3 times on 3 different samples. The average value is shown in Table 2, it should be noted that the difference between the measured values of the 3 samples > 5% will be eliminate.

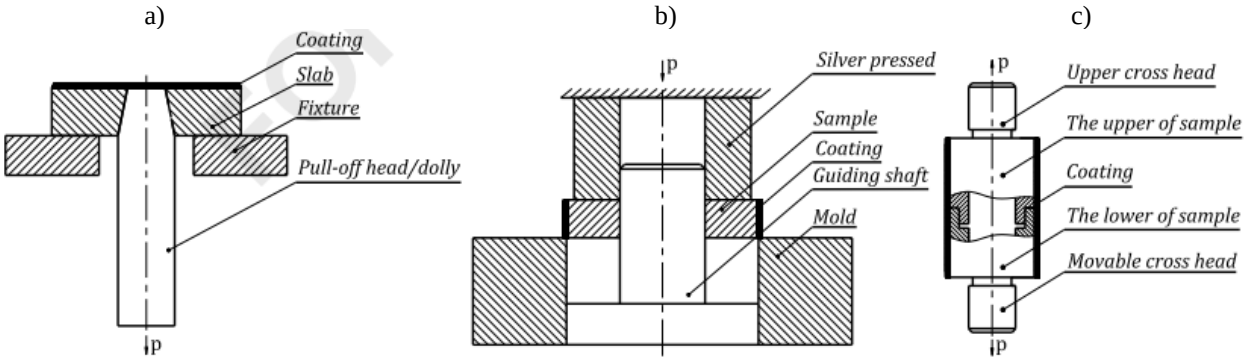

Fig. 2. Schematic diagrams of measurement: a) measurement of adhesion strength, b) measurement of shear adhesion strength, c) measurement of tensile strength

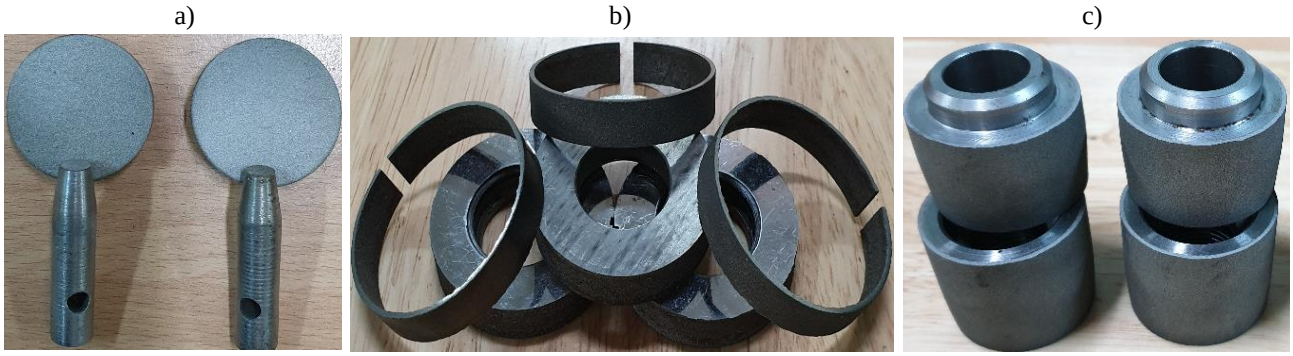

Fig. 3. Samples after measurement: a) dolly is burst out after pulling, b) coating is separated after compression, c) coating is broken

3. RESULT AND DISCUSSION

The coating process for the samples is conducted according to Table 2, the measuring results of each sample for 3 output parameters including (σ_{As}, τ_{Sa} and σ_{Ts}) are also presented in Table 2.

Table 2. Experiment matrix and result

TT	Parameters			Results		
	I_s (A)	m_s (g/min)	L_s (mm)	σ_{As} (MPa)	τ_{Sa} (MPa)	σ_{Ts} (MPa)
1	–1	–1	–1	21.9	36.3	99.4
2	1	–1	–1	33.5	41.6	102.6
3	–1	1	–1	30.6	43.1	107.2
4	1	1	–1	31.8	45.2	111.2
5	–1	–1	1	29.8	41.6	105.5
6	1	–1	1	34.5	46.1	110.7

7	–1	1	1	35.1	43.5	108.2
8	1	1	1	31.9	44.0	115.4
9	–α	0	0	28.3	38.8	100.4
10	+α	0	0	32.5	44.0	109.7
11	0	–α	0	29.6	40.2	101.1
12	0	+α	0	32.1	43.6	110.5
13	0	0	–α	25.5	38.2	98.1
14	0	0	+α	31.7	42.8	108.6
15	0	0	0	38.5	48.5	121,1
16	0	0	0	38.4	49.7	120.4
17	0	0	0	39.2	49.9	120.8
18	0	0	0	38.6	48.0	120.5
19	0	0	0	38.3	51.7	120.2
20	0	0	0	38.0	48.8	119.8
Standard deviations				4.6	4.1	7.7

3.1. ADHESION STRENGTH OF THE COATING AND BASE STEEL

The ANOVA results of the adhesion strength are introduced in Table 3. It is revealed that: in the linear model, the stand-off distance is the most influential (9.89%/21.12% of the contribution), followed by the current intensity (7.89%/21.12%) and powder feed flow is the last (3.34%/21.12%).

Table 3. Results of ANOVA on adhesion strength of the coating and base steel

Source	Degree Freedom (*DF*)	Sum squared deviation (Seq SS)	Contribution to the model	Average squared (Adj MS)	Statistical value (*F*-Value)	Probability value (*P*-Value)
Model	9	411.072	97.02%	45.675	36.12	0.000
Linear	3	89.496	21.12%	29.832	23.59	0.000
I_s	1	33.419	7.89%	33.419	26.43	0.000
m_s	1	14.156	3.34%	14.156	11.19	0.007
L_s	1	41.921	9.89%	41.921	33.15	0.000
Square	3	261.42	61.70%	87.147	68.91	0.000
$I_s{*}I_s$	1	59.188	13.97%	90.347	71.44	0.000
$m_s{*}m_s$	1	60.143	14.19%	79.228	62.65	0.000
$L_s{*}L_s$	1	142.111	33.54%	142.111	112.38	0.000
Interaction	3	60.134	14.19%	20.045	15.85	0.000
$I_s{*}m_s$	1	41.861	9.88%	41.861	33.10	0.000
$I_s{*}L_s$	1	15.961	3.77%	15.961	12.62	0.005
$m_s{*}L_s$	1	2.311	0.55%	2.311	1.83	0.206
Error	10	12.646	2.98%	1.265		
Lack-of-Fit	5	11.846	2.80%	2.369	14.81	0.005
Coefficient of determination R^2: 97.02%						
Adjusted coefficient of determination (R_{adj}^2): 94.33%						

The results in this table shows that the quadratic model has a significant contribution to the model (61.70%), in addition, it can be seen that the probability value (*P*-value) of the all elements in the quadratic model is really small (~0,0001). These values are far from the significance level α (α = 0.05 [27]). This indicates that the appearance of the elements is

considerable for the model. Moreover, the probability value (P~0.005) in Lack-of-Fit test of the regression model is smaller than the significance level (α = 0.05), this means that the model fits the data well. Furthermore, the regression coefficient (R^2) proves that 97.02% of the experimental data are suitable with the predicted data based on the model. $R_{adj}^2 \approx 94.33\%$ matches as well. A quadratic polynomial regression model for predicting the adhesion strength is built as formula (2).

$$\sigma_{As} = -202.6 + 0.4162I_p + 2.981m_p + 0.9064L_p - 0.000250I_{p*}I_p - 0.02344m_{p*}m_p - 0.001963L_{p*}L_p - 0.002288I_{p*}m_p - 0.000353I_{p*}L_p - 0.001344m_{p*}L_p \quad (2)$$

Regression model is applied to predict the adhesion strength, the results of the comparison between the predicted and experimental adhesion strength are introduced and described in Fig. 4.

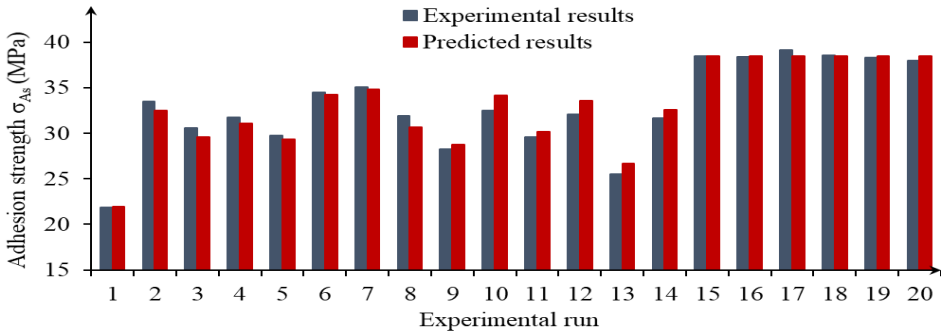

Fig. 4. Comparison between the predicted and experimental adhesion strength

The results indicate that the predicted adhesion strength is nearly close to the measured with 5.1% of the maximum difference and 2.0% of the average difference. Hence, the regression model is tested and able to be applied for predicting the adhesion strength as well as optimizing it.

3.2. SHEAR ADHESION STRENGTH OF THE COATING AND BASE STEEL

Similarly, ANOVA for the shear adhesion strength of the coatings and the base steel listed in Table 2, the results of analysis of variance for the shear adhesion strength are presented in Table 4.

It is clearly revealed that: in the linear model, the current intensity is the parameter that has a greatest impact on the shear adhesion strength of the coating and the base steel (9.66%/21.20%), followed by the stand-off distance (6.05%/21.20%) and finally the powder feed rate (5.48%/21.20%). Observing the results in this Table 4 also shows that the quadratic model has a great contribution to the model of the shear adhesion strength of the coating and base steel (66.38%). Also, the probability value (P-value) of the elements in the quadratic model is extremely small (~0,0001), especially compared to the significance level α. This proves that the appearance of the elements is significant for the model.

Moreover, the probability value (P~0,366) in the Lack-of-Fit test of the regression model is really higher than the significance level α, however the regression coefficient (R^2) shows that 93.85% of the experimental data fit the predicted data from the model. Adjusted coefficient of determination ($R_{adj}^2 \approx 8.32\%$) matches as well. A quadratic polynomial regression model for predicting the adhesion strength of the coatings and base steel is built as formula (3).

Table 4. Results of ANOVA on shear adhesion strength of the coating and base steel

Source	Degree Freedom (DF)	Sum squared deviation (Seq SS)	Contribution to the model	Average squared (Adj MS)	Statistical value (F-Value)	Probability value (P-Value)
Model	9	317.923	93.85%	35.325	16.96	0.000
Linear	3	71.803	21.20%	23.934	11.49	0.001
I_s	1	32.740	9.66%	32.740	15.72	0.003
m_s	1	18.553	5.48%	18.553	8.91	0.014
L_s	1	20.510	6.05%	20.510	9.85	0.011
Square	3	224.874	66.38%	74.958	35.99	0.000
$I_s{*}I_s$	1	57.832	17.07%	85.699	41.14	0.000
$m_s{*}m_s$	1	57.519	16.98%	73.723	35.39	0.000
$L_s{*}L_s$	1	109.523	32.33%	109.523	52.58	0.000
Interaction	3	21.245	6.27%	7.082	3.40	0.062
$I_s{*}m_s$	1	6.480	1.91%	6.480	3.11	0.108
$I_s{*}L_s$	1	0.720	0.21%	0.720	0.35	0.570
$m_s{*}L_s$	1	14.045	4.15%	14.045	6.74	0.027
Error	10	20.829	6.15%	2.083		
Lack-of-Fit	5	12.076	3.56%	2.415	1.38	0.366
Coefficient of determination R^2: 93.85%						
Adjusted coefficient of determination (R_{adj}^2): 88.32%						

$$\tau_{Sa} = -143.1 + 0.3227I_s + 2.498m_s + 0.723L_s - 0.000244I_s{*}I_s - 0.02261m_s{*}m_s - 0.001723L_s{*}L_s - 0.000900I_s{*}m_s - 0.000075I_s{*}L_s - 0.00331m_s{*}L_s \quad (3)$$

Regression model is applied to predict the shear adhesion strength, the results of the comparison between the predicted and experimental shear adhesion strength are introduced and described in Fig. 5.

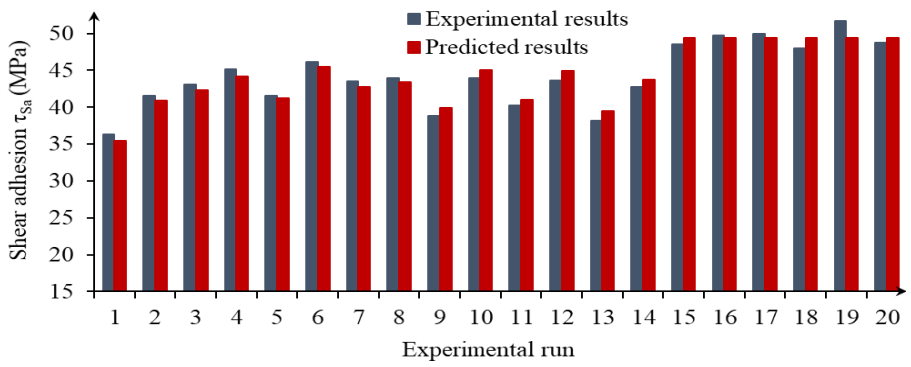

Fig. 5. Comparison between the predicted and experimental shear adhesion strength

The comparison results show that the predicted shear adhesion strength is close to the measured. The maximum difference is 4.5% and the average difference is 2.1%. Thus, the determined regression model is tested and able to be applied for predicting the shear adhesion strength as well as optimizing it.

3.3. TENSILE STRENGTH OF THE COATINGS

ANOVA for the tensile strength of the coatings is displayed in Table 2, the results of analysis of variance are presented in Table 5. The results in this table indicate that: with regard to linear model, the powder feed rate is the most impactful parameter to the tensile strength model (9.60%/25.60%), the second is the stand-off distance, which accounts for 8.40%/25.60% and the last is the current intensity (7.60%/25.60%).

Table 5. Results of ANOVA on tensile strength of the coatings

Source	Degree Freedom (DF)	Sum squared deviation (Seq SS)	Contribution to the model	Average squared (Adj MS)	Statistical value (*F*-Value)	Probability value (*P*-Value)
Model	9	1148.61	95.98%	127.623	26.56	0.000
Linear	3	306.37	25.60%	102.125	21.25	0.000
I_s	1	90.94	7.60%	90.936	18.92	0.001
m_s	1	114.88	9.60%	114.877	23.90	0.001
L_s	1	100.56	8.40%	100.561	20.93	0.001
Square	3	827.75	69.17%	275.916	57.42	0.000
$I_s{*}I_s$	1	210.55	17.60%	312.988	65.13	0.000
$m_s{*}m_s$	1	218.26	18.24%	278.381	57,93	0.000
$L_s{*}L_s$	1	398.93	33.34%	398.928	83.01	0.000
Interaction	3	14.49	1.21%	4.828	1.00	0.430
$I_s{*}m_s$	1	0.98	0.08%	0.980	0.20	0.661
$I_s{*}L_s$	1	3.38	0.28%	3.380	0.70	0.421
$m_s{*}L_s$	1	10.13	0.85%	10.125	2.11	0.177
Error	10	48.06	4.02%	4.806		
Lack-of-Fit	5	47.02	3.93%	9.404	45.51	0.000
Coefficient of determination R^2: 95.98%						
Adjusted coefficient of determination (R_{adj}^2): 92.37%						

Observing the results in this Table 5 also reveals that the quadratic model greatly contributes to the model of the tensile strength of the coating (69.17%). Besides, the probability value (*P*-value) of the elements in the quadratic model is extremely small, especially compared to the significance level α. This proves that the appearance of the elements is considerable for the model.

Moreover, the probability value (*P*~0,0001) in the Lack-of-Fit test of the regression model is higher than the significance level α (<< 0.05), this means that the model fits the data well. Furthermore, the regression coefficient (R^2) proves that 95.98% of the experimental data

are corresponding to the predicted data based on the model. Adjusted coefficient of determination ($R_{adj}^2 \approx 92.37\%$) matches as well. A quadratic polynomial regression model for predicting the tensile strength is built as formula (2).

$$\sigma_{Ts} = -171.5 + 0.5019I_p + 3.184m_p + 1.115L_p - 0.000466I_{p*}I_p - 0.04394m_{p*}m_p \\ -0.003288L_{p*}L_p + 0.000350I_{p*}m_p + 0.000163I_{p*}L_p - 0.00281m_{p*}L_p \quad (4)$$

Regression model is used to predict the tensile strength of the coatings, the results of the comparison between the predicted and experimental tensile strength are introduced and described in Fig. 6.

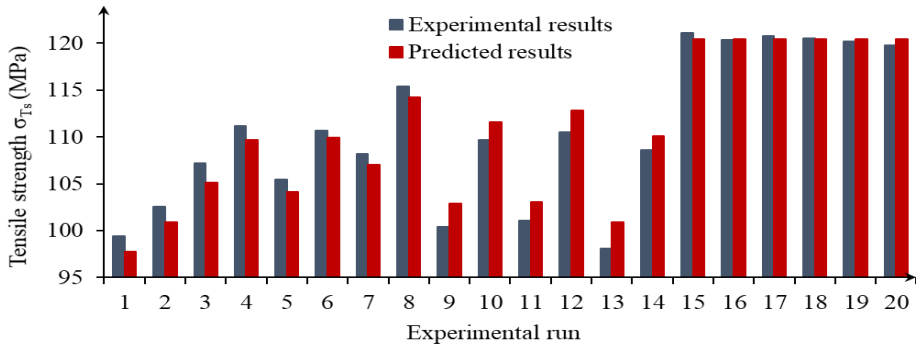

Fig. 6. Comparison between the predicted and experimental tensile strength of the coatings

The results demonstrate that the predicted tensile strength is close to the measured with 2.9% of the maximum difference and 1.2% of the average difference. Consequently, the defined regression model is tested and able to be used for predicting the tensile strength as well as optimizing it.

4. OPTIMIZATION AND EXAMINATION

In a optimizing process, the goal is to achieve the maximum of the adhesion strength, shear adhesion strength and tensile strength (σ_{As}, τ_{Sa} and σ_{Ts}). Minitab 19^{TM} software is used in this process. An optimization graph with the parameters obtained are shown in Fig. 7.

Table 6. Optimization results and experimental verification

Output target	Target	Input parameters when optimizing			Predicted results	Experimental results	Deviations (%)
		I_s (A)	m_s (g/min)	L_s (mm)			
σ_{As} (MPa)	Maximum	575.5	31.2	167.5	38.83	37.97	2.21
τ_{Sa} (MPa)	Maximum				49.78	47.83	3.92
σ_{Ts} (MPa)	Maximum				121.32	118.78	2.10

Experiments for examination are performed with the optimal values of input parameters (I_s, m_s and L_s) in Table 6 after solving the multi-objective optimization problem and

the measurement results are also presented in this table. Similarly to the results in Table 2, all measurements have standard deviations less than 5% and are not showed in this table. The output parameters of the experimental results and predicted results are very close: The coating shear adhesion strength has a largest difference (3.92%), the Tensile strength coatings has a smallest difference (2.10%). Consequently, the optimal values of the parameters obtained are reliable to use.

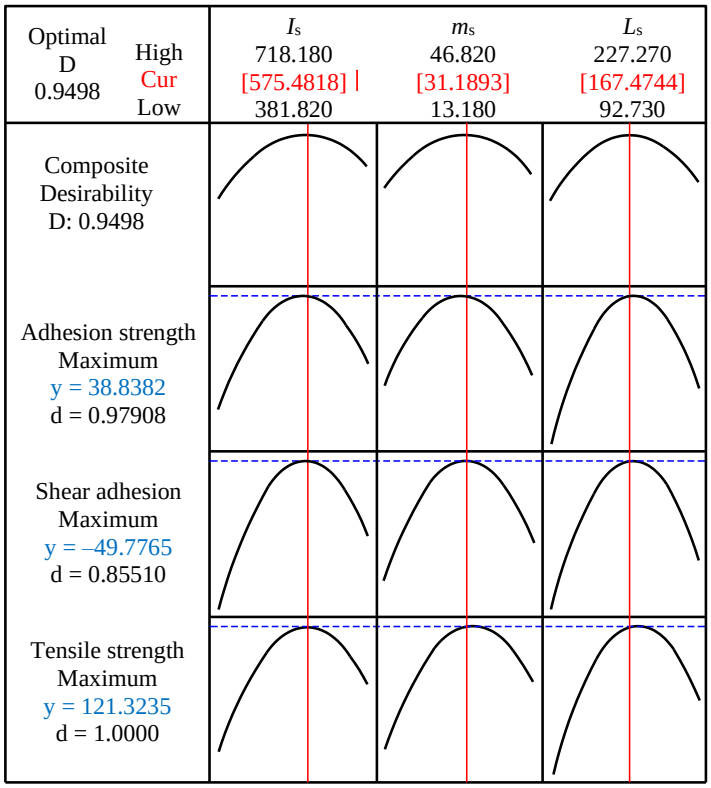

Fig. 7. Multi-objective optimization graph

5. CONCLUSION

In this research, influence of 3 input parameters including I_s, m_s and L_s on the adhesion strength, shear adhesion and tensile strength of the Cr_3C_2-30%NiCr coating fabricated by a plasma spraying on alloy steel E355 (St 52–3)/1.0060 was studied. Optimizing problem was also solved in order to achieve the input parameter with which the adhesion and tensile strength reached the highest values. The analysis results show that the 3 input parameters have a significant effect on the output parameters. In addition, I_s = 575.5 A; m_s = 31.2 g/min and L_s = 167.5 mm are proposed for the coatings with the maximum predicted values, including the achieved adhesion strength of 38.83 MPa, the shear adhesion strength of 49.78 MPa and the tensile strength of 121.32 MPa. The experiments on the verification samples indicated that the measured results are close to the predicted. The degree of agreement of the results between the experiments and prediction is 96.08% at the minimum and 97.90% at the maximum.

ACKNOWLEDGMENTS

This research is supported by Hanoi University of Industry through the science and technology program.

REFERENCES

[1] LI X.M., YANG Y.Y., SHAO T.M., JIN Y.S., BARBEZAT G., 1997, *Impact Wear Performances of Cr_3C_2-NiCr Coatings by Plasma and HVOF-Spraying*, Wear, 202/2, 208–214.

[2] MARCANO Z., LESAGE J., CHICOT D., MESMACQUE G., PUCHI-CABRERA E.S., STAIA M.H., 2008, *Microstructure and Adhesion of Cr_3C_2–NiCr Vacuum Plasma Sprayed Coatings*, Surf. Coat., Technol. 202/18, 4406–4410.

[3] MAGNANI M., SUEGAMA P.H., ESPALLARGAS N., FUGIVARA C.S., DOSTA S., GUILEMANY J.M., BENEDETTI A.V., 2009, *Corrosion and Wear Studies of Cr_3C_2NiCr-HVOF Coatings Sprayed on AA7050 T7 Under Cooling*, J. Therm. Spray Technol. 18, 353–363, https://doi.org/10.1007/s11666-009-9305-6.

[4] YAGHTIN A.H., SALAHINEJAD E., KHOSRAVIFARD A., ARAGHI A., AKHBARIZADEH A., 2015, *Corrosive Wear Behavior of Chromium Carbide Coatings Deposited by Air Plasma Spraying*, Ceram. Int., 41/6, 7916–7920.

[5] ZAVAREH A.M., SARHAN A.A.D.M., RAZAK B.B., BASIRUN W.J., 2015, *The Tribological and Electrochemical Behavior of HVOF-Sprayed Cr_3C_2–NiCr ceramic coating on carbon steel*., Ceram. Int., 41/4, 5387–5396.

[6] VAN T.N., NGUYEN T.A., THU Q.L., HA PHAM THI H.P., 2019, *Influence of Plasma Spraying Parameters on Microstructure and Corrosion Resistance of Cr_3C_2-25NiCr Cermet Carbide Coating*, Anti Corros. Methods Mater. 66, 336–342.

[7] LI J.F., LI L., DING C.X., 2005, *Thermal Diffusivity of Plasma-Sprayed Cr_3C_2–NiCr coatings*, Iranian Journal of Materials Science and Engineering, A394, 229–237.

[8] EL RAYES M., HANY S. ABDO H.S., KHALIL A.K., 2013, *Erosion - Corrosion of Cermet Coating*, Int. J. Electrochem. Sci., 8, 1117–1137.

[9] FEDRIZZI L., VALENTINELLI L., ROSSI S., SEGNA S., 2007, *Tribocorrosion Behaviour of HVOF Cermet Coatings*, Corros. Sci., 49/7, 2781–2799.

[10] DU J.-Y., LI F.-Y., LI Y.-L., WANG L.-M., LU. H.-Y., RAN X.-J., ZHANG X.-Y., 2019, *Influences of Plasma arc Remelting on Microstructure and Service Performance of Cr_3C_2-NiCr/NiCrAl Composite Coating*. Surf. Coat. Technol. 369/15, 16–30.

[11] Thermal Spray Coating Market Analysis, Grand View Research Inc., San Francisco (2015), ISBN Code: 978-1-68038-514-4

[12] WANG Y., HAN Y., LIN C., ZHENG W., JIANG C., WEI A., LIU Y., ZENG Y., SHI Y., 2021, *Effect of Spraying Power on the Morphology of YSZ Splat and Micro-Structure of Thermal Barrier Coating*, Ceramics International, 47/13, 18956–18963, https://doi.org/10.1016/j.ceramint.2021.03.238.

[13] DAVIS J.R., 2004, *Handbook of Thermal Spray Technology*, ASM International, Thermal Spray Society, DAVIS & ASSOCIATES.

[14] CUONG P.D., THAO DX., 2021, *Effect of Surface Roughness and Plasma Current to Adhesion of Cr3C2-NiCr Coating Fabricated by Plasma Spray Technique on 16Mn steel*, International Journal of Modern Physics B., https://doi.org/10.1142/S0217979221400373

[15] MAUER G., VASSEN R., STOEVAR D., KIRNER S., MARQUE´S J-L., ZIMMERMANN S., FORSTER G., SCHEIN J., 2011, *Improving Powder Injectionin Plasma Spraying by Optical Diagnosticsof the Plasma and Particle Characterization*., Journal of Thermal Spray Technology., 20/1–2, 3–11., https://doi.org/10.1007/s11666-010-9577-x.

[16] BISSON J.F., GAUTHIER B., MOREAU C., 2003, *Effect of Plasma Fluctuations on in-Flight Particle Parameters*., J. Therm. Spray Technol., 12/1, 38–43.

[17] DU N.V., BINH N.D., 2011, *Experimental Planning in Engineering*., Hanoi Science and Technology Publishing House.